JOURNAL OF MATERIALS SCIENCE 29 (1994) 3185–3192

Fabrication and mechanical behaviour of Al_2O_3/Mo nanocomposites

M. NAWA
Materials Research and Development Laboratory, Matsushita Electric Works Ltd, 1048, Kadoma, Osaka 571, Japan

T. SEKINO, K. NIIHARA
The Institute of Scientific and Industrial Research, Osaka University, 8-1, Mihogaoka, Ibaraki, Osaka 567, Japan

Two types of Al_2O_3/Mo composites were fabricated by hot-pressing a mixture of γ- or α-Al_2O_3 powder and a fine molybdenum powder. For Al_2O_3/5 vol% Mo composite using γ-Al_2O_3 as a starting powder, the elongated molybdenum layers were observed to surround a part of the Al_2O_3 grains, which resulted in an apparent high value of fracture toughness (7.1 MPa $m^{1/2}$). In the system using α-Al_2O_3 as a starting powder, nanometre sized molybdenum particles were dispersed within the Al_2O_3 grains and at the grain boundaries. Thus, it was confirmed that ceramic/metal nanocomposite was successfully fabricated in the Al_2O_3/Mo composite system. With increasing molybdenum content, the elongated molybdenum particles were formed at Al_2O_3 grain boundaries. Considerable improvements of mechanical properties were observed, such as hardness of 19.2 GPa, fracture strength of 884 MPa and toughness of 7.6 MPa $m^{1/2}$ in the composites containing 5, 7.5, 20 vol% Mo, respectively; however, they were not enhanced simultaneously. The relationships between microstructure and mechanical properties are also discussed.

1. Introduction

Sintered ceramics, due to their desirable properties such as high refractory capability, good wear resistance, and chemical stability, are being investigated as candidates for a wide variety of engineering applications. As opposed to metallic materials, ceramics have inherently strong covalent and ionic bonds that prohibit substantial dislocation motion or plastic deformation. Therefore, most ceramics fail to alleviate stress concentrations that occur in front of a crack tip. Consequently, ceramics are easily fractured as a consequence of crack propagation resulting from a slight surface flaw or internal flaw. Thus, ceramics exhibit poor toughness which restricts their application for structural materials.

To improve the mechanical properties, particularly fracture strength and toughness, many attempts have been made to provide ceramic matrix composites incorporating second-phase dispersions such as particulates, platelets, whiskers or fibres [1–4]. In this case, ceramic/ceramic systems are the most active field of ceramic matrix composite research. On the other hand, there are also some investigations regarding ceramic/metal composites which have incorporated secondary metal-phase dispersions such as tungsten, molybdenum, titanium, chromium, nickel, etc. [5–10]. However, for both types of composites, fracture strength and toughness have not been improved simultaneously. This is mainly due to the fact that the addition of second-phase dispersions generally causes an enlargement of the flaw size in the composites. Therefore, these composites have advanced from a micro-order dispersion to a nano-order dispersion, especially in the ceramic/ceramic systems in an attempt to alleviate this problem. In recent years, nanocomposites, in which nanometre sized second particles are dispersed within the ceramic matrix grains and at the grain boundaries, have shown significant improvements in mechanical properties, such as fracture strength, hardness and creep resistance, even at high temperatures [11–13]. However, with regard to fracture toughness, the ceramic nanocomposites have only shown slight improvement. Consequently, it is highly desirable to further improve the fracture toughness of ceramic nanocomposites so that they may combine excellent toughness with fracture strength.

The purpose of this investigation was to extend nanocomposites to other ceramic/metal composite systems containing nanometre-sized metal inclusions and to confirm the possibility for toughening and strengthening of the ceramic matrix. In the first approach, Al_2O_3 and molybdenum were selected for the ceramic matrix and metal dispersions, respectively. Al_2O_3 has been well examined as a structural ceramic and has been studied in ceramic/ceramic nanocomposite systems such as Al_2O_3/SiC [11, 12]. Molybdenum particles were selected as one of the refractory metals and a material having lower thermal expansion

0022–2461

coefficient than the Al_2O_3 matrix. A conventional powder metallurgical technique was used for preparing Al_2O_3/Mo composites. In the system Al_2O_3/5 vol % Mo composites, γ- and α-phase of Al_2O_3 were used as a starting powder for the matrix, respectively. In Al_2O_3/Mo composites containing above 5 vol % Mo, however, only α-Al_2O_3 powder was used. In this paper, the fabrication process, microstructure and mechanical properties will be described for Al_2O_3/Mo composites containing up to 20 vol % Mo.

2. Experimental procedure

2.1. Fabrication

γ-Al_2O_3 powder (Asahi Chemical Co.) with a specific surface area of 100 $m^2 g^{-1}$ and α-Al_2O_3 powder (Taimei Chemical Co.) with an average particle size below 0.3 μm were used as starting materials for the matrix, respectively. Molybdenum powder (Japan New Metals Co.) with an average particle size of 0.65 μm was used as reinforcing metal particles, but it had a bimodal distribution with the particle size below 0.2 μm and above 1 μm. The powder mixtures, containing 5, 7.5, 10, 15, 20 vol % Mo, were ball milled using zirconia milling media in acetone for 24 h. These slurries were dried and passed through a 250 μm screen. Then the mixtures were hot-pressed in carbon dies of 40 mm diameter. The hot-pressing conditions were 1400°–1700 °C with an applied pressure of 30 MPa for 1 h under a vacuum of less than 10^{-4} torr (1 torr = 133.322 Pa).

2.2. Characterization

Phase identification of the composite was determined by X-ray diffraction analysis on the surfaces of the specimens. The densities of the specimens were obtained by the Archimedes method using toluene as the medium. The microstructure of the composites and the crack propagation behaviour were observed by scanning electron microscopy (SEM). More detailed microstructural characteristics were examined by transmission electron microscopy (TEM). The grain size was estimated by the line intercept method.

2.3. Mechanical properties

The hot-pressed specimens were cut by a diamond-blade saw, and ground with a 600-grit diamond wheel. The specimens had the dimensions of 3 mm × 4 mm × 35 mm for the mechanical properties measurement, and 3 mm × 1 mm × 38 mm for the elastic modulus measurement. The elastic modulus was determined by the resonance vibration method with first-mode resonance. The fracture strength was measured by a three-point bending test at room temperature. The span length and crosshead speed were 20 mm and 0.5 mm min^{-1}, respectively. The tensile surfaces of the specimens were perpendicular to the hot-pressing axis and were polished with a diamond liquid suspension. The fracture toughness was estimated by the indentation fracture (IF) method using the following equation of Marshall and Evans [14]

$$K_{IC} = 0.036E^{0.4} P^{0.6} a^{-0.7} (c/a)^{-1.5} \quad (1)$$

Where E is the elastic modulus and P is an applied load. Here a and c are characteristic dimensions of the Vickers impression and the radial/median crack, respectively. The polished surfaces were used for the Vickers indentation with a load of 196 N and a loading duration of 15 s. The Vickers hardness of the composite was determined separately with a load of 9.8 N.

3. Results and discussion

3.1. Phase identification

In the system of Al_2O_3/5 vol % Mo composite hot-pressed at 1600 °C using γ-Al_2O_3 as a starting powder, mainly α-Al_2O_3 and molybdenum were found, but MoO_2 phase was detected as an oxidized phase. To investigate the cause of the MoO_2 formation during sintering, reduction under hydrogen up to 1200 °C was attempted before hot-pressing for the composite using γ-Al_2O_3 as the starting powder. In this case, the composite hot-pressed in vacuum after hydrogen reduction was composed of only α-Al_2O_3 and molybdenum but no MoO_2. From this result, it was assumed that the formation of MoO_2 was derived from the γ-Al_2O_3 powders possessing high reactivity and hydroxyl groups absorbed on the surfaces of the powder due to the extremely large specific surface area. The relative density of the composite was only 98.5%, probably due to the formation of the MoO_2 phase possessing a lower density than molybdenum.

On the other hand, in the system using α-Al_2O_3 as a starting powder, only α-Al_2O_3 and molybdenum were observed for the composites containing up to 20 vol % Mo hot-pressed at 1400°–1700 °C. These composites obtained relative densities above 99.5%.

3.2. Microstructures

Fig. 1 shows scanning electron micrographs of the fracture surface for Al_2O_3/5 vol % Mo composite hot-pressed at 1600 °C for 1 h under a vacuum, using γ-Al_2O_3 as a starting powder. The elongated molybdenum layers, having an approximate length of 10 μm, were observed to surround a part of the Al_2O_3 grains. The formation of the elongated molybdenum layers was estimated to be related to the formation of MoO_2 phase. It is considered that, during sintering, the surfaces of molybdenum particles are oxidized by hydroxyl groups absorbed around the γ-Al_2O_3 particles to produce molybdenum oxides. In the phase diagram of the Mo–O system [15], molybdenum oxides are known to have various oxide valence levels between MoO_3 and MoO_2 such as Mo_4O_{11} and Mo_9O_{26}. In addition, there are many liquid phases that coexist such as MoO_2 + liquid, MoO_3 + liquid, Mo_4O_{11} + liquid, and Mo_9O_{26} + liquid. In particular, the MoO_2 + liquid phase has a wide range above 818 °C. Therefore, it seems reasonable to assume that the formation of the elongated molybdenum layers was derived from a liquid phase, such as MoO_2 + liquid.

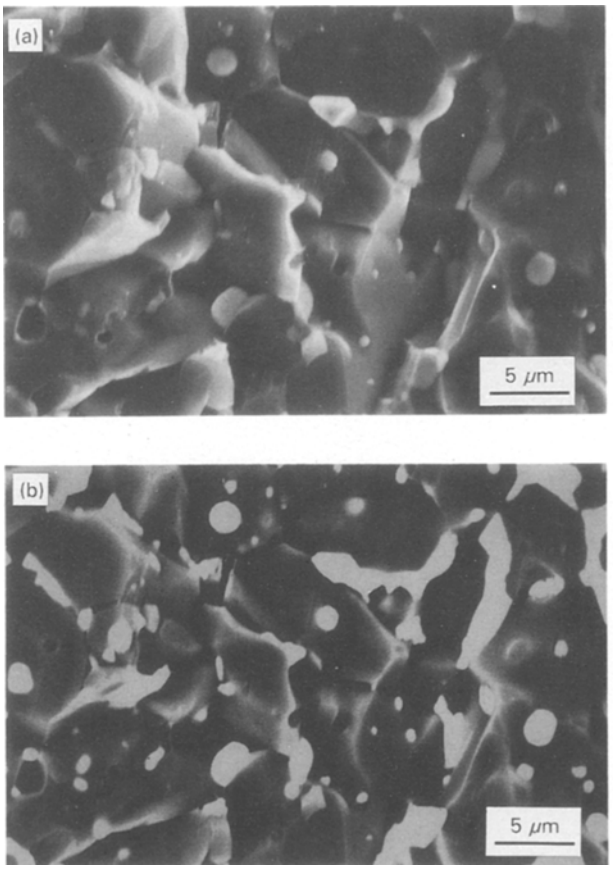

Figure 1 Scanning electron micrographs of the fracture surface for Al_2O_3/5 vol % Mo composite fabricated using γ-Al_2O_3 as a starting powder: (a) hot-pressed at 1660 °C, (b) back-scattered electron image of (a).

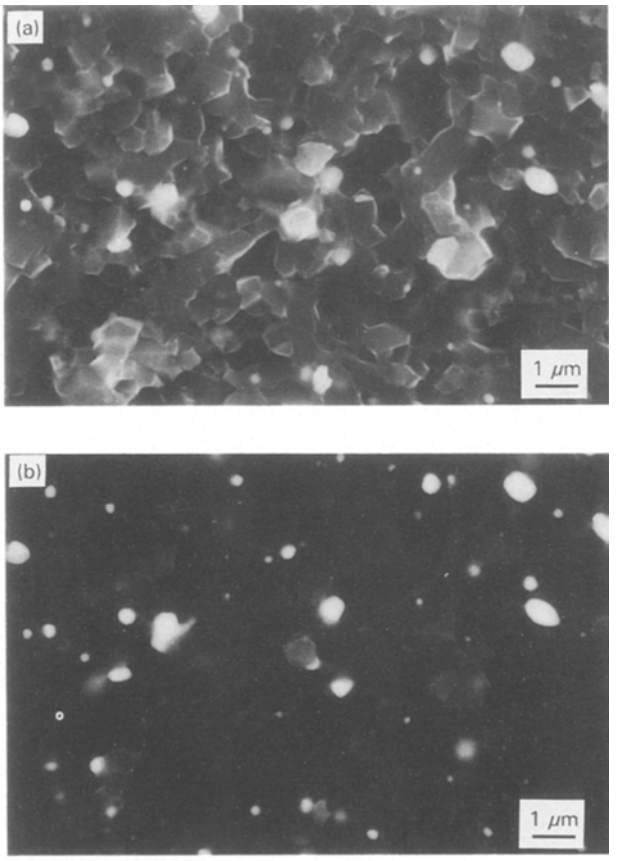

Figure 2 Scanning electron micrographs of the fracture surface for Al_2O_3/5 vol % Mo composite fabricated by using α-Al_2O_3 as a starting powder: (a) hot-pressed at 1600 °C, (b) back-scattered electron image of (a).

The Al_2O_3 grains grew to columnar form having an approximate length of 15 μm and an average grain size of 8–9 μm, probably due to the formation of a liquid phase associated with the formation of the MoO_2. The particle size of spherical molybdenum was less than 2 μm. Smaller sized molybdenum particles, less than 1 μm, were observed within the Al_2O_3 matrix grains.

Fig. 2 shows scanning electron micrographs of the fracture surface for Al_2O_3/5 vol % Mo composite hot-pressed at 1600 °C for 1 h under a vacuum, using α-Al_2O_3 as a starting powder. The fine microstructure of Al_2O_3/Mo composite was determined to have an average grain size of less than 1 μm. This was much smaller than the grain size of the composite which used γ-Al_2O_3 as a starting powder. The variation of the average grain size with hot-pressing temperature is shown in Fig. 3. It was shown that the addition of molybdenum particles, which served as inclusions, resulted in grain-growth inhibition of the Al_2O_3 matrix. However, with increasing molybdenum content and rising sintering temperature, slight grain growth of Al_2O_3 and the coalescence of molybdenum particles at the Al_2O_3 grain boundaries were observed.

Typical TEM image of Al_2O_3/5 vol % Mo composite hot-pressed at 1500 °C, using α-Al_2O_3 as a starting powder, are shown in Fig. 4. The nanometre-sized molybdenum particles were confirmed to be dispersed within the equiaxed Al_2O_3 matrix grains and at the grain boundaries. In addition, the larger

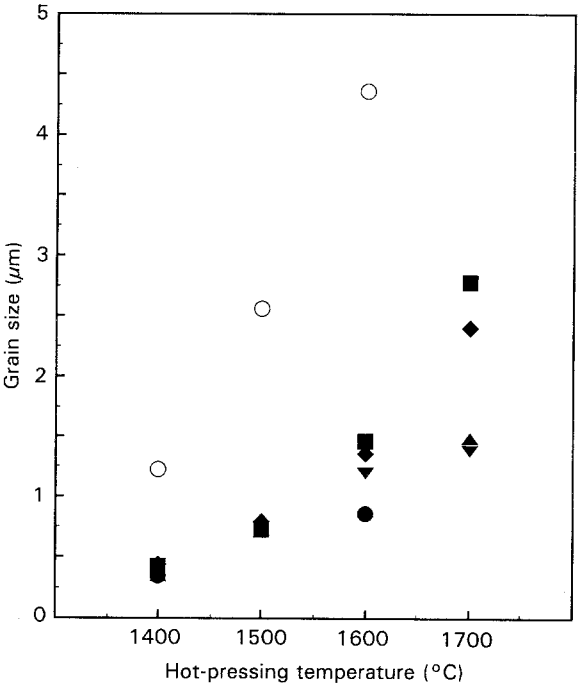

Figure 3 Variation of average grain size with hot-pressing temperature for Al_2O_3/Mo composites. (○) Monolithic Al_2O_3, (●) Al_2O_3/5 vol % Mo, (▲) Al_2O_3/7.5 vol % Mo, (▼) Al_2O_3/10 vol % Mo, (◆) Al_2O_3/15 vol % Mo, (■) Al_2O_3/20 vol % Mo.

molybdenum particles, above 1 μm, appeared to be located at the grain boundaries. Furthermore, as shown in Fig. 5, no reaction phase was observed at the interface between Al_2O_3 and molybdenum within the

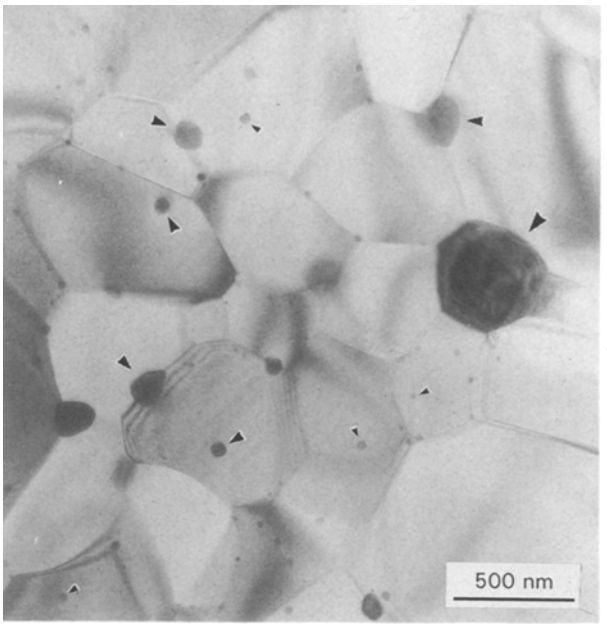

Figure 4 TEM image of the microstructure for Al_2O_3/5 vol % Mo composite fabricated by hot-pressing under a vacuum.

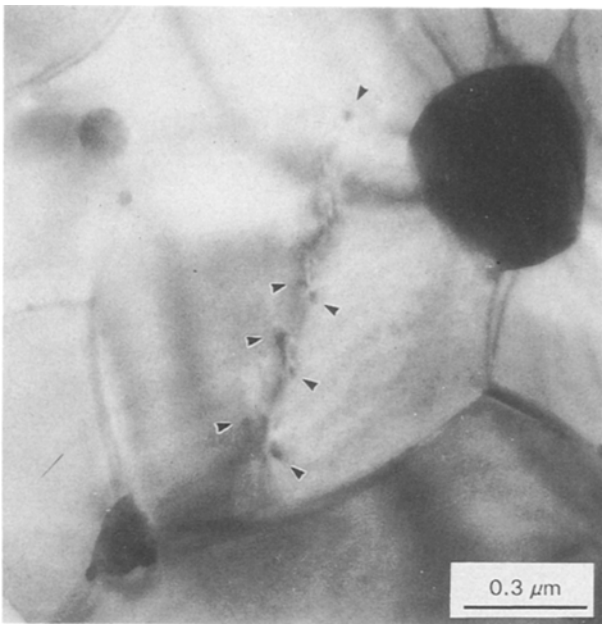

Figure 6 A line of piled up dislocation observed within the Al_2O_3 for Al_2O_3/5 vol % Mo composite.

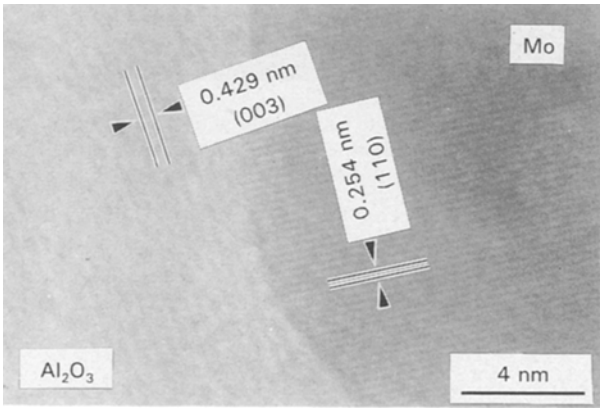

Figure 5 High-resolution TEM image of the interface between Al_2O_3 matrix and molybdenum within the Al_2O_3 grain.

Al_2O_3 grain. The composite prepared in this work, therefore, had a mixed morphology composed of both intragranular and intergranular microstructural features. Consequently, it was confirmed that ceramic/metal nanocomposite was successfully fabricated in the Al_2O_3/Mo composite system when α-Al_2O_3 was used as a starting powder.

Fig. 6 shows what seems to be a line of piled up dislocations within the Al_2O_3 grain for Al_2O_3/5 vol % Mo composite. The formation of a dislocation might be regarded as one argument in support of the existence of localized internal stresses within the Al_2O_3 grains and/or around the molybdenum particles caused from their thermal expansion mismatch.

3.3. Mechanical properties

For Al_2O_3/5 vol % Mo composite hot-pressed at 1600 °C, using γ-Al_2O_3 as a starting powder, fracture strength was 306 MPa which was much lower than that of the monolithic Al_2O_3 prepared under the same conditions. As shown in Fig. 7, characteristic crack-

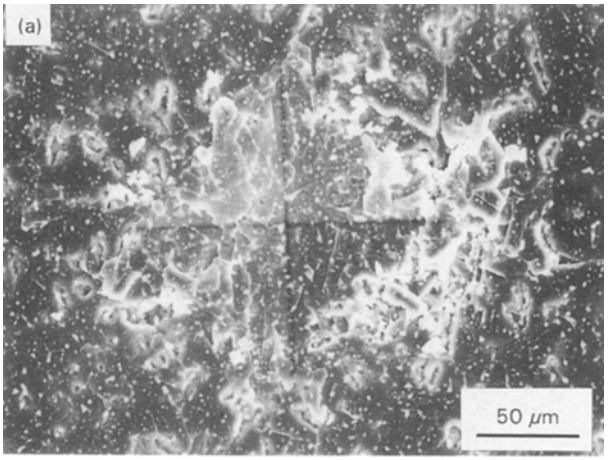

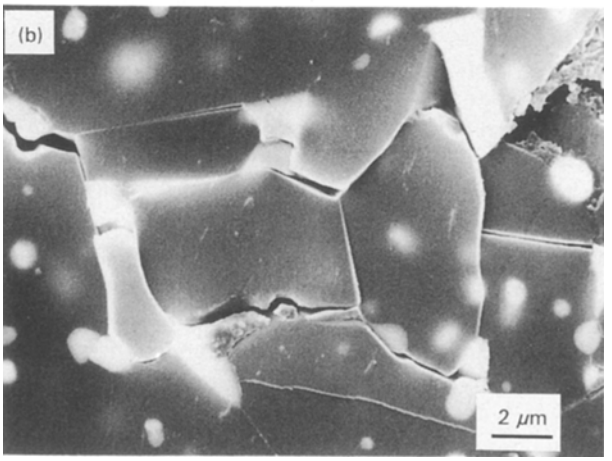

Figure 7 Scanning electron micrographs of the crack-type morphology around the Vickers indentation for Al_2O_3/5 vol % Mo composite fabricated by using γ-Al_2O_3 as a starting powder: (a) entire indentation, (b) isolated cracks.

type morphology around the Vickers indentation was observed. It was shown that many cracks branched and propagated between various Al_2O_3 grains and the interfaces of the elongated molybdenum layers. These results suggest that the grain boundaries of Al_2O_3 and interfaces of elongated molybdenum layers are fairly weak. In addition, for the composite containing coalesced and elongated molybdenum particles in the Al_2O_3 matrix composed of developed columnar microstructure, there is a fear of the production of microcracking due to the crystal anisotropy of the thermal expansion coefficient of Al_2O_3 and the thermal expansion mismatch between Al_2O_3 and molybdenum, in the case where the dimension of the molybdenum particles exceeds the critical particle size for microcracking. However, it was ascertained that there were no traces of microcracks by SEM observations. Hence, the lower fracture strength of the composite was supposed to be contributed to the weak grain boundaries between the interfaces of elongated molybdenum layers and Al_2O_3 grains, along with the grain growth of Al_2O_3 matrix.

On the other hand, in the composite having a microstructure described above, fracture toughness could not be evaluated by the IF method; therefore, the single-edge precracked beam (SEPB) method [16] was tried to estimate an approximate value. In the SEPB method, the half size specimens from the fracture strength test were used in a three-point bending test with a span length of 16 mm. Fracture toughness evaluated by the SEPB method was 7.1 MPa $m^{1/2}$. In addition, as shown in Fig. 7b, there was some evidence that cracks propagated through the elongated molybdenum layers. Therefore, it was supposed that fracture toughness was improved by incorporating metal phase associated with a relaxation of stress intensity derived from bridging of the crack tip by the elongated molybdenum layers, although the contribution of microcrack toughening could not be completely excluded.

Next, the mechanical properties of Al_2O_3/Mo composites, using α-Al_2O_3 as a starting powder, are described below. Fig. 8 shows the variation of fracture strength with hot-pressing temperature for the Al_2O_3/Mo composites containing up to 20 vol % Mo. On the whole, fracture strength was increased by the addition of molybdenum particles; however, it decreased with increasing hot-pressing temperature for both monolithic Al_2O_3 and Al_2O_3/Mo composites containing molybdenum content. Fracture strength of the Al_2O_3/7.5 vol % Mo composite hot-pressed at 1400 °C exhibited a maximum value of 884 MPa, which was 1.5 times larger than that of the monolithic Al_2O_3 prepared under the same conditions. When the hot-pressing temperature was increased to 1700 °C, strength decreased to around 450 MPa, which corresponded to the grain growth of Al_2O_3 matrix. Thus, in the Al_2O_3/Mo composites, strengthening was assumed to be mainly attributed to the inhibition of grain growth of Al_2O_3 matrix in the presence of nanometre-sized molybdenum particles. Scanning electron micrographs of fracture surfaces for monolithic Al_2O_3 and Al_2O_3/7.5 vol % Mo composites are shown in Figs 9 and 10, respectively. As shown in Fig. 10, the microstructure of the Al_2O_3/7.5 vol % Mo composites, hot-pressed at any temperature, was composed of relatively equiaxed Al_2O_3 matrix grains. However, many voids were observed, in which relatively large molybdenum particles seemed to be pulling out from the grain boundaries or triple junctions of the Al_2O_3. This result suggests that the bonding strength of the interfaces between Al_2O_3 grains and molybdenum particles is not strong. On the other hand, the fracture mode of monolithic Al_2O_3 was mainly intergranular, as shown in Fig. 9, but in the case of a large grain size, transgranular fracture mode was observed. On the contrary, the fracture mode of the composites were predominantly transgranular even in the case of a small grain size. This significant change in fracture mode from intergranular

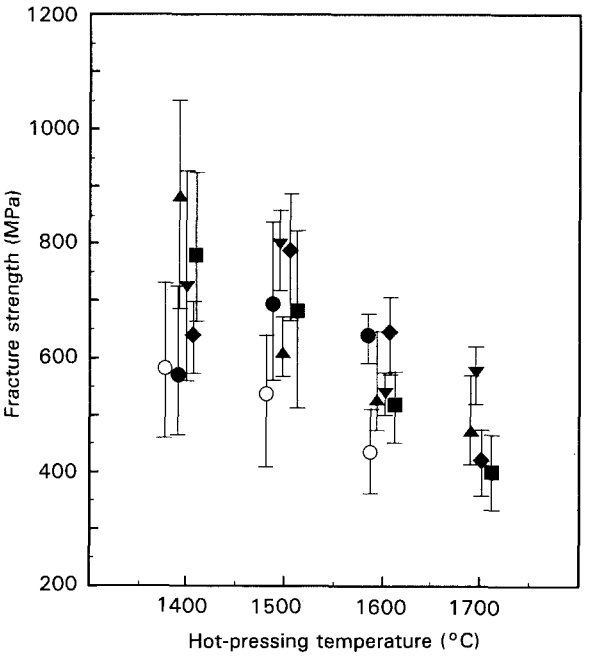

Figure 8 Variation of fracture strength with hot-pressing temperature for Al_2O_3/Mo composites. (○) Monolithic Al_2O_3, (●) Al_2O_3/5 vol % Mo, (▲) Al_2O_3/7.5 vol % Mo, (▼) Al_2O_3/10 vol % Mo, (◆) Al_2O_3/15 vol % Mo, (■) Al_2O_3/20 vol % Mo.

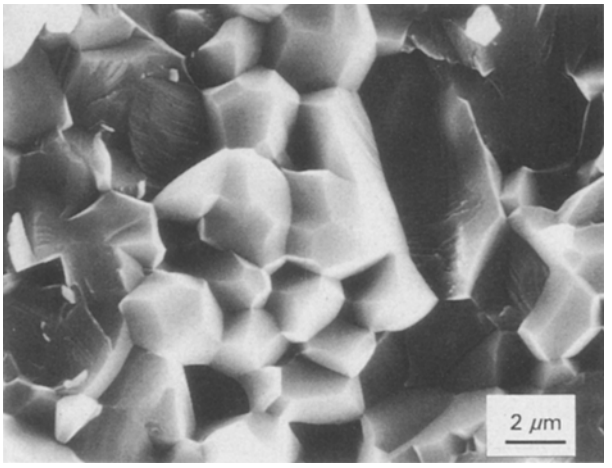

Figure 9 Scanning electron micrograph of the fracture surface for monolithic Al_2O_3 sample hot-pressed at 1500 °C.

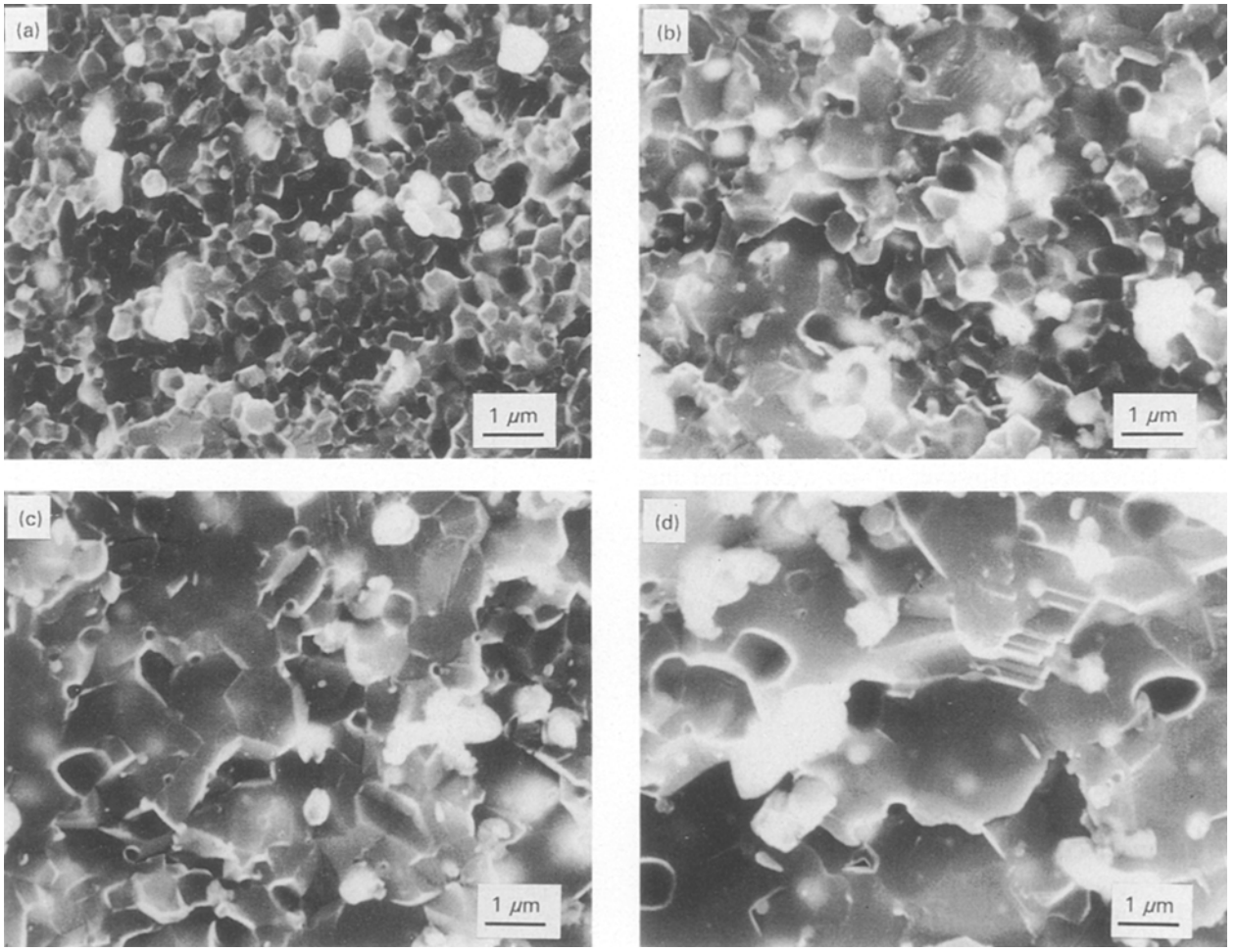

Figure 10 Scanning electron micrographs of the fracture surfaces for Al_2O_3/7.5 vol % Mo composite hot pressed at (a) 1400 °C, (b) 1500 °C, (c) 1600 °C, (d) 1700 °C.

for the monolithic Al_2O_3 to transgranular for the Al_2O_3/Mo composites, may be associated with the internal stresses supposed to be developed during cooling from the sintering temperature because of the thermal expansion mismatch between Al_2O_3 and molybdenum. In the case where molybdenum has a lower thermal expansion coefficient than Al_2O_3, it is proposed that hydrostatic pressures are produced within the molybdenum particle and radial compressive and tangential tensile hoop stresses are also produced around molybdenum particles. Therefore, transgranular fracture for the Al_2O_3/Mo composites was assumed to be derived from crack attraction towards the inner part of the Al_2O_3 grains which is caused by the tangential tensile hoop stresses around the molybdenum particles within the Al_2O_3 grains.

The variation of fracture toughness with molybdenum content for the Al_2O_3/Mo composites is shown in Fig. 11. When hot-pressed at a lower sintering temperature of 1400 °C, fracture toughness for the Al_2O_3/Mo composites was around 4.4 MPa $m^{1/2}$, nevertheless, with increasing molybdenum content up to 20 vol %, which was nearly equal to that of the monolithic Al_2O_3. On the contrary, significant improvement of fracture toughness was observed with increasing molybdenum content and rising hot-pressing temperature. Fracture toughness of the Al_2O_3/20 vol % Mo composite hot-pressed at 1700 °C exhibited a maximum value of 7.6 MPa $m^{1/2}$,

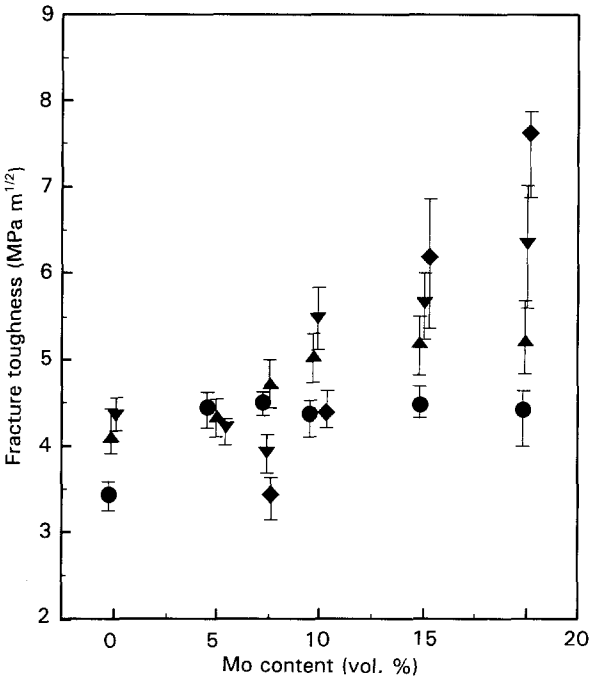

Figure 11 Variation of fracture toughness with molybdenum content for Al_2O_3/Mo composites hot-pressed at (●) 1400 °C, (▲) 1500 °C, (▼) 1600 °C, (◆) 1700 °C.

which was 1.8 times larger than that of the monolithic Al_2O_3 hot-pressed at 1600 °C. The crack propagation behaviour around the Vickers indentation for the Al_2O_3/15 vol % Mo composites hot-pressed in the

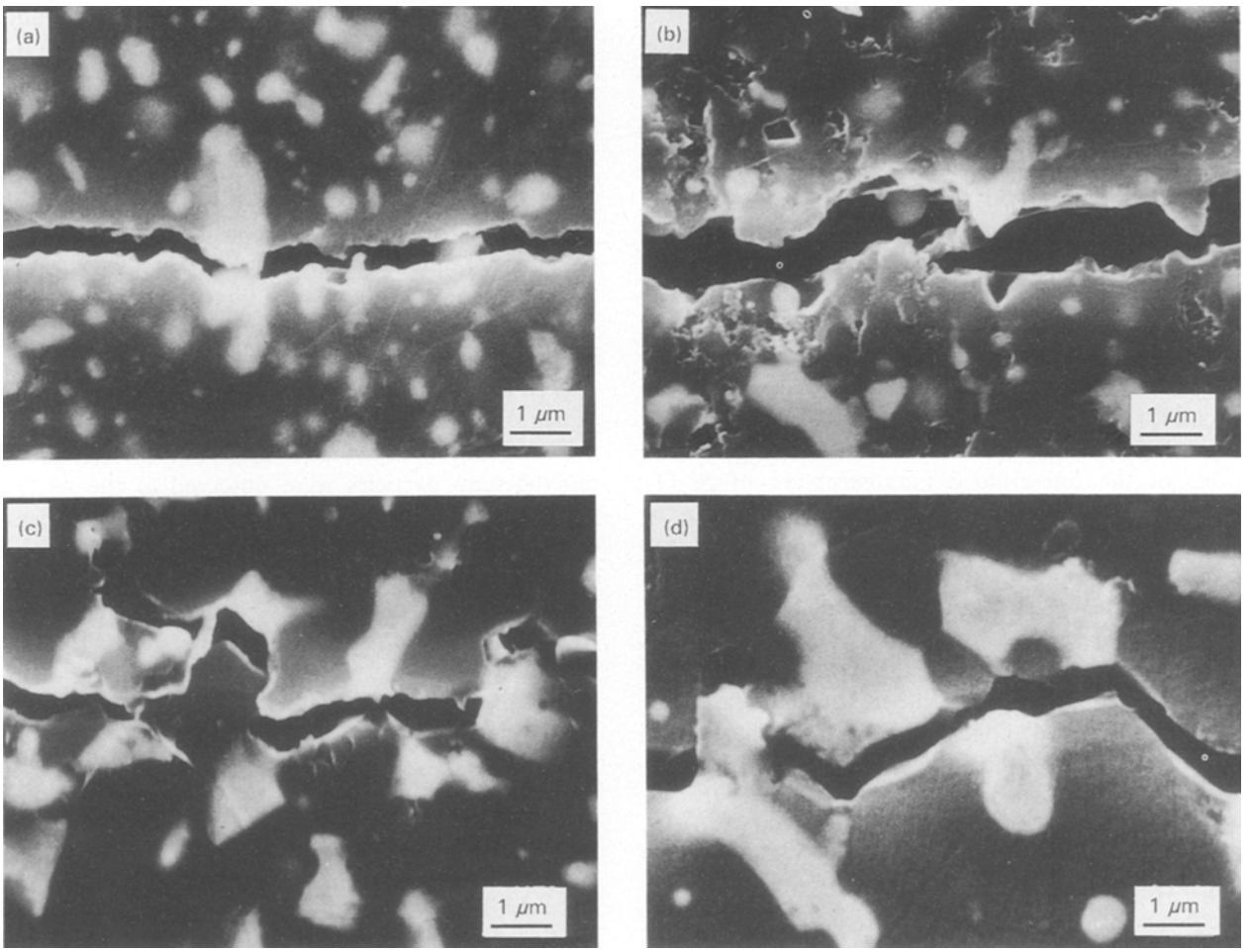

Figure 12 Scanning electron micrographs of the crack propagation behaviour around the Vickers indentation for Al_2O_3/15 vol % Mo composites hot-pressed at (a) 1400 °C, (b) 1500 °C, (c) 1600 °C, (d) 1700 °C.

range 1400°–1700 °C, is shown in Fig. 12. At a lower hot-pressing temperature of 1400 °C, the crack propagated straight with small deviations around relatively small-sized molybdenum particles, which corresponded to the low fracture toughness. While, with increasing hot-pressing temperature, the coalescence of molybdenum particles and the formations of elongated molybdenum particles, which were formed due to the necking of molybdenum particles, were observed at the Al_2O_3 grain boundaries. As a whole, cracks propagated with large deflection around coalesced molybdenum particles. In addition, predominant evidence of crack penetration behaviour through the elongated molybdenum particles and crack-bridging by the metal phase were observed, which corresponded to the significant improvement of fracture toughness. These interactions between crack tip and metal phase were assumed to be due to the stress shielding effect acting as a toughening mechanism, which is based on the relaxation of stress intensity derived from blunting and/or bridging of crack tip by the metal phase, and plastic deformation which occurs when cracks penetrate through the elongated molybdenum particles.

Fig. 13 shows the variation of the Vickers hardness with molybdenum content for the Al_2O_3/Mo composites. The dotted line represents hardness calculated by the linear rule of mixtures, where the hardness of monolithic Al_2O_3 and molybdenum polycrystal is

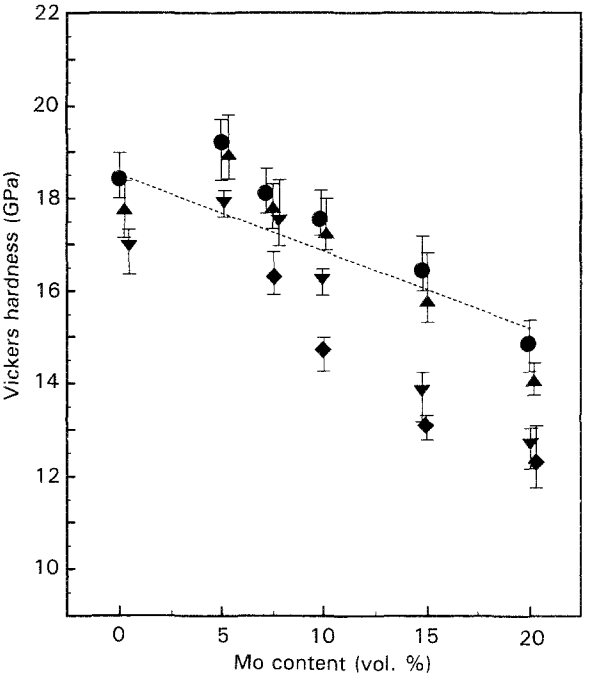

Figure 13 Variation of Vickers hardness with molybdenum content for Al_2O_3/Mo composites hot-pressed at (●) 1400 °C, (▲) 1500 °C, (▼) 1600 °C, (◆) 1700 °C.

18.5 and 2.1 GPa [17], respectively. On the whole, the hardness of the Al_2O_3/Mo composites decreased with increasing molybdenum content, which approximately obeyed the rule of mixtures. In addition, a

decrease of hardness was also observed with increasing hot-pressing temperature for both monolithic Al_2O_3 and Al_2O_3/Mo composites containing individual molybdenum contents. This decrease in hardness was thought to be attributable to the coalesced and elongated molybdenum particles at the Al_2O_3 grain boundaries and the grain growth of Al_2O_3 matrix. However, for the composites containing 5–15 vol % Mo hot-pressed at lower sintering temperatures, higher values of hardness than those predicted by the rule of mixtures were observed. Furthermore, the Al_2O_3/5 vol % Mo composites exhibited obvious hardening and obtained a maximum value of 19.2 GPa when hot-pressed at 1400 °C. This hardening is supposed to be accounted for by the contributions of the fine-grained microstructure of Al_2O_3 matrix [18] and/or the intergranular nanostructure of Al_2O_3/Mo composites, in which nanometre-sized molybdenum particles are dispersed within the Al_2O_3 grains and at the grain boundaries. In fact, the monolithic Al_2O_3 prepared in this work showed a negative dependence of grain size on the hardness, as clearly seen in Fig. 13 and the nanometre-sized metal particle will cause the hardening itself [19]. In another aspect related to the intergranular nanostructure, the radial compressive stresses around molybdenum particles within the Al_2O_3 grains, which are assumed to be generated by their thermal expansion mismatch, might cause the hardening of Al_2O_3 grains. Therefore, it is proposed that these contributions will result in the higher hardness values observed.

4. Conclusions

Two types of Al_2O_3/Mo composites were fabricated by hot-pressing a mixture of γ- or α-Al_2O_3 powder and a fine molybdenum powder under a vacuum using a conventional powder metallurgical process. The microstructure and mechanical properties were examined for both Al_2O_3/Mo composites. The results are summarized as follows.

1. Al_2O_3/5 vol % Mo composite using γ-Al_2O_3 as a starting powder was composed of mainly α-Al_2O_3 and molybdenum, but MoO_2 was detected as an oxidized phase. The composite had a microstructural feature in which the elongated molybdenum layers, that were assumed to be formed due to the formation of liquid phase, surrounded a part of the Al_2O_3 grains. Many cracks were observed branching and propagating between various Al_2O_3 grains and interfaces of the elongated molybdenum layers. Fracture toughness exhibited an apparently high value, although no enhancement of fracture strength was observed.

2. Al_2O_3/5–20 vol % Mo composites using α-Al_2O_3 as a starting powder were composed of only α-Al_2O_3 and molybdenum. In these composites, nanometre-sized molybdenum particles were dispersed within the Al_2O_3 grains and relatively large molybdenum particles, above 1 μm, were located at the grain boundaries. Thus, it was confirmed that ceramic/metal nanocomposites were successfully fabricated. TEM observation revealed that no reaction phases were present at the interfaces between the Al_2O_3 and molybdenum within the Al_2O_3 grains.

3. The addition of molybdenum particles resulted in the grain-growth inhibition of the Al_2O_3 matrix. The fracture strength of Al_2O_3/7.5 vol % Mo composite hot-pressed at 1400 °C was 884 MPa, which was 1.5 times larger than that of the monolithic Al_2O_3. The fracture mode of the composites was confirmed to be predominantly transgranular. Higher values of hardness than those predicted by the rule of mixtures were observed for the composites hot-pressed at lower sintering temperatures.

4. With increasing molybdenum content and rising hot-pressing temperature, the coalescence of molybdenum particles and the formation of the elongated molybdenum particles were observed at the Al_2O_3 grain boundaries. Predominant evidence of crack penetration behaviour through the elongated molybdenum particles and crack-bridging by the metal phase were observed. The fracture toughness of Al_2O_3/20 vol % Mo composite hot-pressed at 1700 °C was 7.6 MPa $m^{1/2}$, which was 1.8 times larger than that of the monolithic Al_2O_3.

References

1. N. CLAUSSEN, J. STEEB and R. F. PABST, *Am. Ceram. Soc. Bull.* **56** (1977) 559.
2. T. UCHIYAMA, K. NIIHARA and T. HIRAI, *Yogyo Kyokaishi* **94** (1986) 756.
3. P. F. BECHER and G. C. WEI, *J. Am. Ceram. Soc.* **67** (1984) C267.
4. K. M. PREWO, J. J. BRENNAN and G. K. LAYDEN, *Am. Ceram. Soc. Bull.* **65** (1986) 305.
5. P. HING, *Sci. Ceram.* **10** (1980) 521.
6. C. O. McHUGH, T. J. WHALEN and M. HUMENIK Jr, *J. Am. Ceram. Soc.* **49** (1966) 486.
7. D. T. RANKIN, J. J. STIGLICH, D. R. PETRAK and R. RUH, *ibid.* **54** (1971) 277.
8. Y. NAERHEIM, *Powder Metall. Int.* **18** (1986) 158.
9. S. A. CHO, M. PUERTA, B. COLS and J. C. OHEP, *ibid.* **12** (1980) 192.
10. E. BREVAL, G. DODDS and C. G. PANTANO, *Mater. Res. Bull.* **20** (1985) 1191.
11. K. NIIHARA, A. NAKAHIRA, T. UCHIYAMA and T. HIRAI, in "Fracture Mechanics of Ceramics 7", edited by R. C. Bradt, A. G. Evans, D. P. H. Hasselman and F. F. Lange (Plenum Press, New York, 1986) p. 103.
12. K. NIIHARA, A. NAKAHIRA, G. SASAKI and M. HIRABAYASHI, in "Proceeding of MRS Meeting on Advanced Materials" (Plenum, Tokyo, 1988) p. 129.
13. K. NIIHARA, *J. Ceram. Soc. Jpn* **99** (1991) 974.
14. D. B. MARHALL and A. G. EVANS, *J. Am. Ceram. Soc.* **64** (1981) C-182.
15. ERNEST M. LEVIN and HOWARD F. McMURDIE, "Phase diagrams for ceramists" (American Ceramic Society, Columbus, OH, 1975) Fig. 4158.
16. T. NOSE and T. FUJII, *J. Am. Ceram. Soc.* **71** (1988) 328.
17. C. S. SMITHELLS, "Metals References Book", Vol. 3 (Butterworths, London, 1967) p. 917.
18. P. M. SARGENT and T. F. PAGE, *Proc. Br. Ceram. Soc.* **26** (1978) 209.
19. P. E. WIERENGA, A. G. DIRKS and J. J. BROEK, *Thin Solid Films* **119** (1984) 375.

Received 25 June
and accepted 16 December 1993